Catalysis Today 164 (2011) 320–324

Contents lists available at ScienceDirect

Catalysis Today

journal homepage: www.elsevier.com/locate/cattod

Au–Pd alloying-promoted thermal decomposition of PdO supported on SiO_2 and its effect on the catalytic performance in CO oxidation

Kun Qian, Weixin Huang*

Hefei National Laboratory for Physical Sciences at the Microscale and Department of Chemical Physics, University of Science and Technology of China, Jinzhai Road 96, Hefei 230026, China

ARTICLE INFO

Article history:
Available online 1 November 2010

Keywords:
Au–Pd alloy
PdO
H_2-TPR
XPS
CO oxidation

ABSTRACT

We have prepared a series of Au–Pd/SiO_2 catalysts by the routine deposition–precipitation method followed by calcination at 200 °C in air for 4 h. The structures of these catalysts have been characterized with powder X-ray diffraction, transmission electron microscopy, X-ray photoelectron spectroscopy and H_2-temperature-programmed reduction. Their catalytic activity in CO oxidation has also been studied. We found that the preparation procedure leads to the formation of highly dispersed PdO supported on SiO_2 in Pd/SiO_2, but to the formation of both highly dispersed PdO and Au_xPd alloy nanoparticles in Au–Pd/SiO_2 catalysts. The fraction of metallic Pd in Pd species increases with the increase of Au:Pd molar ratio in Au–Pd/SiO_2 catalysts. We proposed that the alloying of Au and Pd can promote the thermal decomposition of PdO supported on SiO_2. Because of the existence of metallic Pd, Au–Pd/SiO_2 catalysts are more active in CO oxidation than Pd/SiO_2. Au–Pd/SiO_2-0.5 exhibits the same activity as Pd/SiO_2-H_2 in CO oxidation. Our results provide some novel information on the fabrication of supported Au_xPd alloy nanoparticles.

1. Introduction

Bimetallic catalysts usually exhibit advantageous properties compared to those of their individual constituent metals [1]. Supported Au–Pd bimetallic catalysts have been reported to show very nice catalytic performance in acetoxylation of ethylene to vinyl acetate [2], direct synthesis of hydrogen peroxide from H_2 and O_2 [3], oxidation of benzyl alcohol, 1-butanol, 2-butanol, 2-buten-1-ol and 1,4-butanediol [4], hydrogenation reaction [5], CO oxidation [6], photocatalysis [7]. It is generally accepted that the synergistic effect exists in the bimetallic catalysts to modify the geometric and the electronic properties of the active site, increase the resistance to particle sintering, and eventually improve the catalytic performance. The structure and synergistic effect of supported Au–Pd bimetallic catalysts have also been much investigated. Hou et al. [4] found that bimetallic Au–Pd nanoparticles with a Au:Pd atomic ratio of 1:3 show a higher catalytic activity than bimetallic Au–Pd nanoparticles with other Au:Pd atomic ratios in oxidation of benzyl alcohol, 1-butanol, 2-butanol, 2-buten-1-ol and 1,4-butanediol. Edwards et al. [8] reported that acid pretreatment of a carbon support for Au–Pd alloy catalysts switches off the decomposition of H_2O_2 by decreasing the size of alloy nanoparticles. Chen et al. [9] revealed that the role of Au in Au–Pd alloy for acetoxylation of ethylene to vinyl acetate is to isolate single Pd sites to facilitate the formation of active sites consisting of two noncontiguous and suitably spaced Pd monomers. Gao et al. [10] proposed that contiguous Pd sites on the AuPd (1 0 0) alloy surface provide O_{ads} and Au and Pd sites provide CO_{ads} so that low-temperature CO oxidation can occur more facilely on supported Au–Pd alloy nanoparticles than on supported Au or Pd nanoparticles. It is interesting that the support was reported to affect the synergistic effect in Au–Pd alloy nanoparticles. Guczi et al. observed a slight synergistic effect for Au–Pd alloy nanoparticles supported on TiO_2 in CO oxidation [6], but no synergistic effect for Au–Pd alloy nanoparticles supported on SiO_2 [11]. Therefore, the synergistic effect in supported Au–Pd alloy catalysts acts in different ways for different catalytic reactions and thus needs further investigation.

The preparation method of supported Au–Pd alloy catalysts is of great importance for the investigation of synergistic effect. Incipient wetness method, deposition–precipitation method, sol-immobilization method, and electroless deposition method that were all followed by H_2 reduction at high temperatures have been employed to synthesize supported Au–Pd alloy catalysts [2–8,11–17]. We consider that the deposition–precipitation method is very suitable for the preparation of supported Au–Pd bimetallic catalysts for the synergistic effect investigation because it does not introduce any other undesired ions and compounds in the catalysts. Meanwhile, our previous studies [18–20] demon-

* Corresponding author. Tel.: +86 551 3600435; fax: +86 551 3600437.
E-mail address: huangwx@ustc.edu.cn (W. Huang).

0920-5861/$ – see front matter © 2010 Elsevier B.V. All rights reserved.
doi:10.1016/j.cattod.2010.10.018

strate that SiO_2 is an appropriate support for the investigation of structure–activity of supported nanoparticles because SiO_2 does not participate in the catalytic reaction. Therefore, in our studies of synergistic effect of supported Au–Pd bimetallic catalysts, we chose SiO_2 as the support and employ deposition–precipitation to prepare the catalysts. In this paper, we report the results of Au–Pd/SiO_2 catalysts prepared by deposition–precipitation followed by calcination at 200 °C in air for 4 h. Very interestingly, such a preparation procedure leads to the formation of highly dispersed PdO supported on SiO_2 in Pd/SiO_2, but to the formation of both highly dispersed PdO and Au_xPd alloy nanoparticles in Au–Pd/SiO_2 catalysts. The fraction of metallic Pd in Pd species increases with the increase of Au:Pd molar ratio in Au–Pd/SiO_2 catalysts. We proposed that the alloying of Au and Pd can promote the thermal decomposition of PdO supported on SiO_2. Because of the existence of metallic Pd, Au–Pd/SiO_2 catalysts are more active in CO oxidation than Pd/SiO_2. Au–Pd/SiO_2-0.5 exhibits the same activity as Pd/SiO_2-H_2 in CO oxidation. Our results provide some novel information on the fabrication of supported Au_xPd alloy nanoparticles.

2. Experimental

A series of supported Au–Pd catalysts with different Au:Pd molar ratios (denoted as Au–Pd/SiO_2-*x*, *x* is the Au:Pd molar ratio) were prepared by the traditional deposition–precipitation method employing $HAuCl_4{\cdot}4H_2O$ (Sinopharm Chemical Reagent Co., Ltd, Au content ≥ 47.8%) and H_2PdCl_4 (Sinopharm Chemical Reagent Co., Ltd., $PdCl_2$:HCl molar ratio: 1:2) as the precursors and inert SiO_2 (40–120 mesh, Qingdao Haiyang Chemicals Co.) as the support. The loading of Pd in the catalysts was fixed with a Pd:SiO_2 weight ratio of 1% in all catalysts. Typically, calculated amounts of $HAuCl_4$ and H_2PdCl_4 aqueous solution were co-added into a three-neck bottle containing the support and adequately stirred, and then ammonia water was slowly added to adjust the pH between 9 and 10. The system was adequately stirred at 60 °C for 24 h. Then the precipitate was filtered and washed several times, and the resulting powder was dried at 60 °C for 12 h followed by calcination in air at 200 °C for 4 h. For comparisons, Au/SiO_2 catalyst with the same Au loading as that in Au–Pd/SiO_2-1 was prepared in a similar way; and Au–Pd/SiO_2 catalysts (denoted as Au–Pd/SiO_2-*x*-H_2) was prepared in a similar way but were finally reduced in H_2 at 200 °C for 4 h.

Powder X-ray diffraction (XRD) patterns were acquired on a Philips X'Pert Pro Super X-ray diffractometer with a Ni-filtered Cu Kα X-ray source operating at 40 kV and 50 mA. Transmission electron microscopy (TEM) measurements were carried out on a JEOL-2100F transmission electron microscope at an accelerating voltage of 200 kV. High resolution X-ray photoelectron spectroscopy (XPS) measurements were performed on an ESCALAB 250 high performance electron spectrometer using monochromatized Al Kα excitation source ($h\nu$ = 1486.6 eV). The binding energies in the XPS spectra were referenced to the Si 2p binding energy in SiO_2 at 103.3 eV. The reduction behavior of Au–Pd/SiO_2 catalysts was measured by H_2 temperature programmed reduction (H_2-TPR). 50 mg catalyst was placed in a quartz reactor and heated at a rate of 10 °C/min. 5% H_2 balanced with Ar was fed at a flow rate of 20 ml/min and the consumption of H_2 was measured by a thermal conductivity detector (TCD).

The catalytic activity of catalysts towards CO oxidation was evaluated with a fixed-bed flow reactor. The catalyst experienced no pre-treatment prior to the catalytic reaction. The used catalyst weight was 100 mg and the reaction gas consisting of 1% CO and 99% dry air was fed at a rate of 20 ml/min. The steady-state composition of the effluent gas was analyzed with an online GC-14C gas chromatograph equipped with a TDX-01 column (T = 80 °C, H_2 as the carrier gas at 30 ml/min). The conversion of CO was calculated from the change in CO concentrations in the inlet and outlet gases.

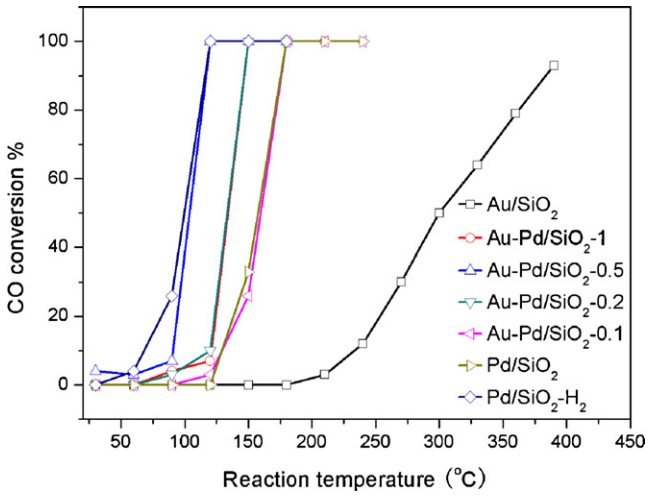

Fig. 1. Catalytic performance of Au–Pd/SiO_2 catalysts in CO oxidation.

3. Results and discussion

Fig. 1 shows the catalytic performances of various Au–Pd/SiO_2 catalysts in CO oxidation. Au/SiO_2 prepared by deposition–precipitation exhibits a poor activity and becomes active at reaction temperatures above 200 °C, in consistence with our previous results [21]. Pd/SiO_2 becomes active at reaction temperatures above 120 °C and acquires a 100% CO conversion at 180 °C, and Pd/SiO_2-H_2 is more active, becoming active at reaction temperatures above 60 °C and acquires a 100% CO conversion at 120 °C. The addition of Au in Pd/SiO_2 promotes its activity in CO oxidation, and the promotion effect depends on the Au:Pd molar ratio. T_{50} (temperature for a 50% CO conversion) was adopted to compare the activity of various Au–Pd/SiO_2 and corresponding Au–Pd/SiO_2-H_2 catalysts, whose results are shown in Fig. 2. Au–Pd/SiO_2-*x*-H_2 ($x \leq 0.5$) exhibits a similar activity to Pd/SiO_2-H_2, and Au–Pd/SiO_2-1-H_2 is less active. The activity of Au–Pd/SiO_2-*x* exhibits a volcano-shape dependence on the *x* value. Au–Pd/SiO_2-0.5 shows the best catalytic activity and its T_{50} is 105 °C. Interestingly, although Pd/SiO_2-H_2 is much more active than corresponding Pd/SiO_2, the difference in the T_{50} between Au–Pd/SiO_2-*x* and corresponding Au–Pd/SiO_2-*x*-H_2 decreases with

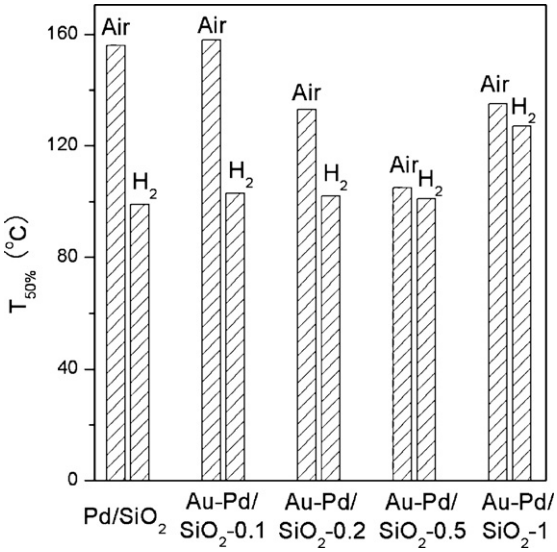

Fig. 2. T_{50} of Au–Pd/SiO_2 and Au–Pd/SiO_2-H_2 catalysts in CO oxidation.

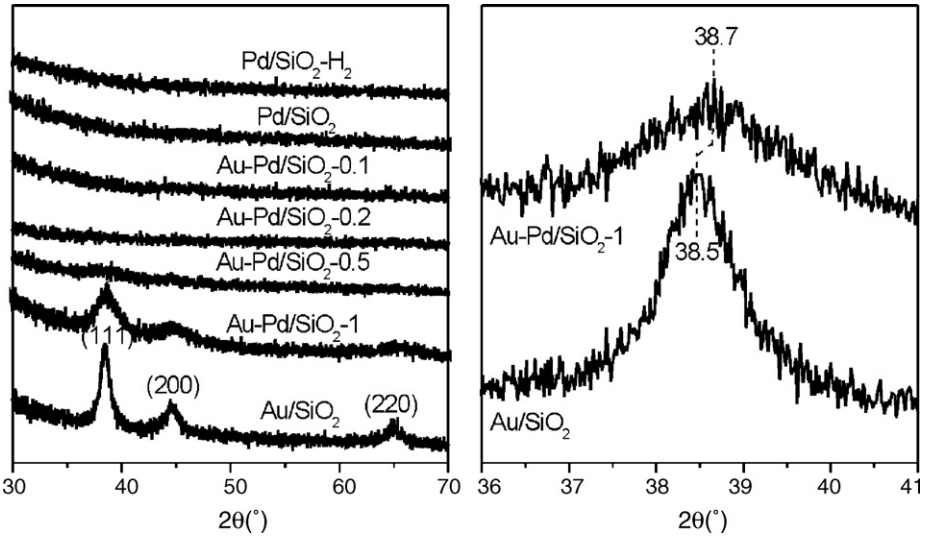

Fig. 3. XRD patterns of Au–Pd/SiO_2 catalysts (left) and the enlarged XRD patterns of Au/SiO_2 and Au–Pd/SiO_2-1 between 36 and 41° (right).

the increase of x value. Au–Pd/SiO_2-x (x = 0.5 and 1.0) exhibits similar T_{50} to corresponding Au–Pd/SiO_2-x-H_2 although Au–Pd/SiO_2-x was prepared by calcination in air while Au–Pd/SiO_2-x-H_2 was prepared by reduction in H_2.

Fig. 3 displays the XRD patterns of various catalysts. No obvious diffraction patterns appears in the XRD spectra of Pd/SiO_2-H_2, Pd/SiO_2, and Au–Pd/SiO_2-x (x = 0.1, 0.2, and 0.5), demonstrating that the Pd and Au species in these catalysts are highly dispersive. Au/SiO_2 shows a typical diffraction pattern arising from Au. The diffraction pattern of Au–Pd/SiO_2-1 is similar to that of Au/SiO_2, but the diffraction peaks of Au–Pd/SiO_2-1 are much broader than those of Au/SiO_2. A careful examination shows that the position of (1 1 1) diffraction peak of Au–Pd/SiO_2-1 (2θ = 38.7°) is distinctly larger than that of Au/SiO_2 (2θ = 38.5°). The same trend also occurs for other diffraction peaks. The standard positions of Au (1 1 1) and Pd (1 1 1) diffraction peaks locate at 38.2 and 39.9°, respectively, therefore, the observed position of (1 1 1) diffraction peak in Au–Pd/SiO_2-1.0 might indicate the formation of Au–Pd alloy, agreeing with previous reports [22,23]. According to the Scherrer equation, the average crystalline size of Au nanoparticles in Au/SiO_2 and Au–Pd alloy nanoparticles in Au–Pd/SiO_2-1 was estimated to be ~10 and ~4 nm, respectively. Fig. 4 shows TEM images of Au/SiO_2, Au–Pd/SiO_2-1 and Pd/SiO_2, in which Au nanoparticles between 7 and 12 nm are clearly visible in Au/SiO_2 whereas no obvious particles could be identified in Pd/SiO_2. TEM results clearly demonstrate the existence of aggregates consisting of fine nanoparticles between 3 and 5 nm in Au–Pd/SiO_2-1, and the HRTEM image reveals a lattice fringe of 0.230 nm for these fine nanoparticles that could be assigned to the lattice fringe of (1 1 1) plane of Au–Pd alloy nanoparticles.

The Pd 3d and Au 4f XPS spectra are shown in Figs. 5 and 6, respectively. Since the Au $4d_{5/2}$ binding energy is similar to the Pd $3d_{5/2}$, therefore we analyzed the Pd 3d XPS spectrum with the Pd $3d_{3/2}$ peak. Pd/SiO_2 exhibits a single Pd $3d_{3/2}$ component with the binding energy at 342.3 eV that can be attributed to PdO whereas Pd/SiO_2-H_2 exhibits a single Pd $3d_{3/2}$ component with the binding energy at 341.2 eV that can be attributed to metallic Pd [22,23]. Therefore, highly dispersive Pd nanoparticles in Pd/SiO_2-H_2 is much more active than highly dispersive PdO nanoparticles in Pd/SiO_2 in CO oxidation reaction, agreeing with the results from surface science studies of model Pd surfaces [24]. Interestingly, although Au–Pd/SiO_2 catalysts were prepared with the same method as Pd/SiO_2, the Pd $3d_{3/2}$ peaks of Au–Pd/SiO_2 catalysts all exhibit two components with the binding energy at 341.2 and 342.3 eV, and the fraction of component at 341.2 eV gradually increases with the increase of Au:Pd molar ratio. These observations demonstrate that the Au additive promotes the thermal decomposition of PdO nanoparticles supported on SiO_2 to form metallic Pd, which is a very interesting result.

The same preparation procedure for Pd/SiO_2 leads to the preparation of metallic Au nanoparticles supported on SiO_2, as demonstrated by the Au $4f_{7/2}$ binding energy of Au/SiO_2 at 84.0 eV. The Au 4f XPS results also show that there is only metallic Au in Au–Pd/SiO_2-1, Au–Pd/SiO_2-0.5 and Au–Pd/SiO_2-0.2. However, the Au $4f_{7/2}$ binding energy shifts from 84.0 eV for Au–Pd/SiO_2-1 to 83.9 eV for Au–Pd/SiO_2-0.5 and 83.8 eV for Au–Pd/SiO_2-0.2, sug-

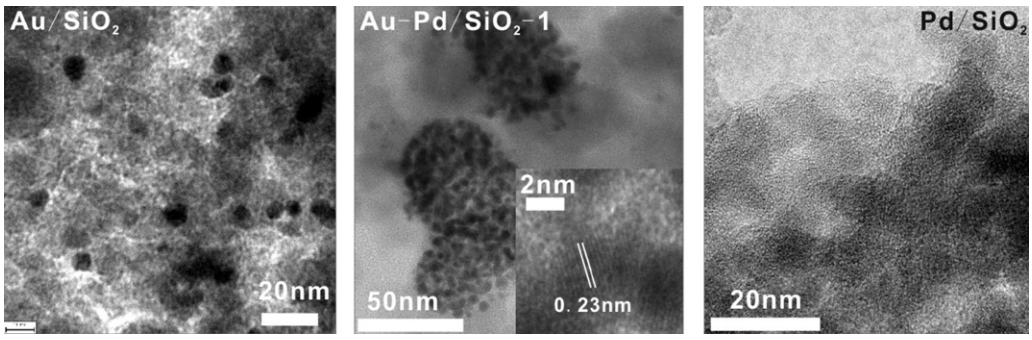

Fig. 4. TEM images of Au/SiO_2, Au–Pd/SiO_2-1 and Pd/SiO_2. The inset shows the HRTEM of Au–Pd/SiO_2-1.

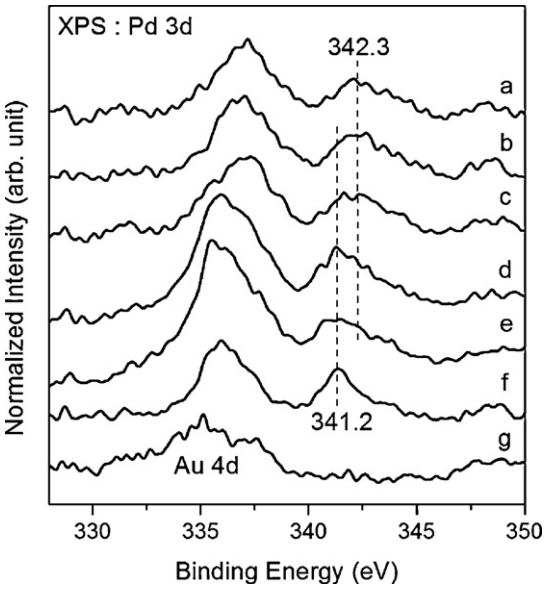

Fig. 5. Pd 3d and Au $4d_{5/2}$ XPS spectra of Pd/SiO_2 (a), $Au–Pd/SiO_2$-0.1 (b), $Au–Pd/SiO_2$-0.2 (c), $Au–Pd/SiO_2$-0.5 (d), $Au–Pd/SiO_2$-1 (e), Pd/SiO_2-H_2 (f), and Au/SiO_2 (g).

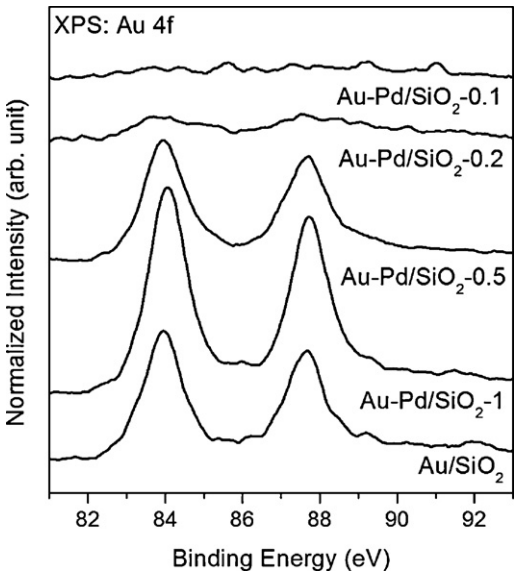

Fig. 6. Au 4f XPS spectra of $Au–Pd/SiO_2$ and Au/SiO_2 catalysts.

gesting that the charge transfer to metallic Au occurs in $Au–Pd/SiO_2$ catalysts and becomes more profound with the decrease of Au:Pd molar ratio. An interesting observation is the variation of Au 4f XPS peak intensity of $Au–Pd/SiO_2$ catalysts. $Au–Pd/SiO_2$-0.1 actually shows no obvious Au 4f XPS peak and $Au–Pd/SiO_2$-0.2 only displays a weak and diffuse Au 4f XPS peak, then $Au–Pd/SiO_2$-0.5 shows a strong Au 4f XPS peak and the intensity of Au 4f peak for $Au–Pd/SiO_2$-1 is nearly as twice as that of $Au–Pd/SiO_2$-0.5. Since XPS is a surface-sensitive method, the intensity variation of Au 4f XPS peak might indicate that Au–Pd alloy nanoparticles in $Au–Pd/SiO_2$-0.5 and $Au–Pd/SiO_2$-1 are more surface-enriched with Au than those in $Au–Pd/SiO_2$-0.1 and $Au–Pd/SiO_2$-0.2. It could also be seen that the Au 4f XPS peak of $Au–Pd/SiO_2$-1 is much more intense than that of Au/SiO_2 although both catalysts have the same Au loading. This agrees with the XRD results that nanoparticles in $Au–Pd/SiO_2$ are much more dispersive than those in Au/SiO_2.

The thermal decomposition of PdO nanoparticles supported on SiO_2 promoted by Au additive is further by the H_2-TPR experimental results (Fig. 7(a)). No reduction peak was observed for Au/SiO_2 catalyst, in consistence with XRD and XPS results that only metallic Au nanoaprticles exist in Au/SiO_2. Pd/SiO_2 shows a broad reduction peak ranging from 100 to 600 °C, which could be assigned to the reduction of PdO nanoparticles interacting with SiO_2 with different interaction strengths [25]. PdO nanoparticles weakly interacting with SiO_2 are reduced at low temperatures. The reduction peak in the H_2-TPR keep decreasing with the increase of Au:Pd molar ratio in $Au–Pd/SiO_2$ catalysts. It is noteworthy that $Au–Pd/SiO_2$-1 exhibits two distinct reduction peaks at 370 and 430 °C although it shows the lowest H_2 consumption, suggesting the enhanced interaction of PdO with SiO_2. Fig. 7(b) shows the H_2 reduction peak areas of $Au–Pd/SiO_2$ catalysts normalized with Pd/SiO_2, clearly demonstrating the fraction of PdO species in $Au–Pd/SiO_2$ catalysts decreases with the increase of Au:Pd molar ratio. From the PdO fraction and Au:Pd molar ratio, the molar ratio of metallic Au:metallic Pd can be calculated to be 1.5, 0.9, 0.4 and 0.3 for $Au–Pd/SiO_2$-1, $Au–Pd/SiO_2$-0.5, $Au–Pd/SiO_2$-0.2 and $Au–Pd/SiO_2$-0.1, respectively.

The XPS and H_2-TPR results clearly evidence that prepared with the same procedure, Pd/SiO_2 only contains PdO whereas $Au–Pd/SiO_2$ catalysts contain both metallic Pd and PdO and the fraction of Pd increases with the increase of Au:Pd molar ratio in

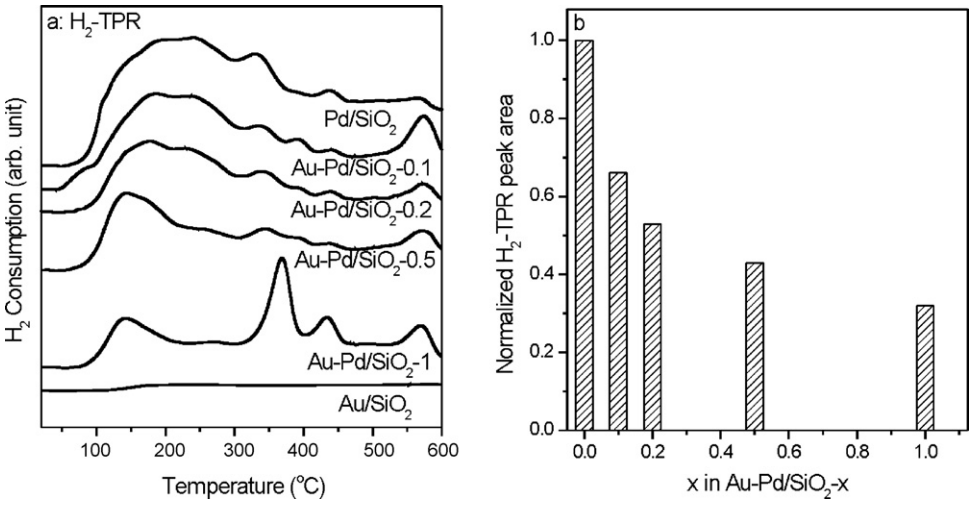

Fig. 7. H_2-TPR profiles (a) and normalized H_2-TPR peak areas (b) of $Au–Pd/SiO_2$ catalysts.

the catalysts. Au/SiO_2 containing only metallic Au nanoparticles can be prepared under the same condition; therefore, we propose the following reaction occurs during the course of calcination of $Au–Pd/SiO_2$ catalysts at 200 °C in air:

$$2xAu + 2PdO \rightarrow 2Au_xPd(alloy) + O_2$$

The alloying of Au and Pd is an exothermal reaction and thus can facilitate the thermal decomposition of PdO supported on SiO_2. Without the alloying process, PdO supported on SiO_2 cannot decompose when calcined at 200 °C in air. The formation of Au_xPd alloy nanoparticles in $Au–Pd/SiO_2$ catalysts is also supported by the observed shift of Au 4f binding energy. The XRD results suggest that the Au_xPd alloy nanoparticles tend to be highly dispersed on SiO_2 with the decrease of Au:Pd molar ratio in the catalysts, which could be attributed to the strong interaction between Pd and SiO_2.

The composition of various $Au–Pd/SiO_2$ catalysts could be estimated from the fraction of PdO (H_2-TPR results) and the Au:Pd molar ratio in Au–Pd alloy nanoparticles. With the same preparation method, the acquired species supported on SiO_2 is highly dispersed PdO in Pd/SiO_2, 66% highly dispersed PdO and 34% highly dispersed $Au_{0.3}Pd$ alloy nanoparticles in $Au–Pd/SiO_2$-0.1, 53% highly dispersed PdO and 47% highly dispersed $Au_{0.4}Pd$ alloy nanoparticles in $Au–Pd/SiO_2$-0.2, 43% highly dispersed PdO and 57% highly dispersed $Au_{0.9}Pd$ alloy nanoparticles in $Au–Pd/SiO_2$-0.5, and 32% highly dispersed PdO and 68% $Au_{1.5}Pd$ alloy nanoparticles with an average crystalline size of 4 nm in $Au–Pd/SiO_2$-1. On basis of the catalytic performance of Pd/SiO_2-H_2, Pd/SiO_2 and Au/SiO_2, it could be concluded that highly dispersed Pd nanoparticles supported on SiO_2 are most active in CO oxidation, therefore, the composition and structure of $Au–Pd/SiO_2$ catalysts can well account for their catalytic performance in CO oxidation. Although the amount of metallic Pd in $Au–Pd/SiO_2$-0.5 is 59% of that in Pd/SiO_2-H_2, $Au–Pd/SiO_2$-0.5 exhibits nearly the same activity in CO oxidation as Pd/SiO_2-H_2. This indicates the existence of a synergistic effect between Au and Pd in $Au_{0.9}Pd$ alloy nanoparticles in $Au–Pd/SiO_2$-0.5 for CO oxidation, as previously observed in CO oxidation over Au–Pd model catalysts [10,26,27]. Comparing $Au_{0.9}Pd$ alloy nanoparticles in $Au–Pd/SiO_2$-0.5, the poor activity of $Au_{1.5}Pd$ alloy nanoparticles in $Au–Pd/SiO_2$-1 could be attributed to both their poor dispersion and the likely Au-enriched surface of $Au_{1.5}Pd$ alloy nanoparticles. The detailed surface structures of Au–Pd alloy nanoparticles are needed for a comprehensive understanding of their catalytic performance in CO oxidation, which are still under investigation.

4. Conclusion

$Au–Pd/SiO_2$ catalysts have been prepared by the routine deposition–precipitation method followed by calcination at 200 °C in air for 4 h. This preparation procedure leads to the formation of highly dispersed PdO supported on SiO_2 in Pd/SiO_2, but to the formation of both highly dispersed PdO and Au_xPd alloy nanoparticles in $Au–Pd/SiO_2$ catalysts. The fraction of metallic Pd in Pd species increases with the increase of Au:Pd molar ratio in $Au–Pd/SiO_2$ catalysts. We proposed that the alloying of Au and Pd can promote the thermal decomposition of PdO supported on SiO_2. Because of the existence of metallic Pd, $Au–Pd/SiO_2$ catalysts are more active in CO oxidation than Pd/SiO_2. $Au–Pd/SiO_2$-0.5 exhibits the same activity as Pd/SiO_2-H_2 in CO oxidation. Our results provide some novel information on the fabrication of supported Au_xPd alloy nanoparticles.

Acknowledgements

This work was financially supported by National Natural Science Foundation of China (grant 20973161), the Ministry of Science and Technology of China (2010CB923302), the MOE program for PCSIRT (IRT0756), and the MPG-CAS partner group program.

References

[1] J.H. Sinfelt, Acc. Chem. Res. 10 (1977) 15.
[2] E.G. Allison, G.C. Bond, Catal. Rev. 7 (1972) 233.
[3] J.K. Edwards, B.E. Solsona, P. Landon, A.F. Carley, A. Herzing, C.J. Kiely, G.J. Hutchings, J. Catal. 236 (2005) 69.
[4] W.B. Hou, N.A. Dehm, R.W.J. Scott, J. Catal. 253 (2008) 22.
[5] W. Juszczyk, Z. Karpinski, D. Lomot, J. Pielaszek, J.W. Sobczak, J. Catal. 151 (1995) 67.
[6] L. Guczi, A. Beck, A. Horváth, Zs. Koppány, G. Stefler, K. Frey, I. Sajó, O. Geszti, D. Bazin, J. Lynch, J. Mol. Catal. A: Chem. 204–205 (2003) 545.
[7] Y. Mizukoshi, K. Sato, T.J. Konno, N. Masahashi, Appl. Catal. B 94 (2010) 248.
[8] J.K. Edwards, B. Solsona, E. Ntainjua N, A.F. Carley, A.A. Herzing, C.J. Kiely, G.J. Hutchings, Science 323 (2009) 1037.
[9] M.S. Chen, D. Kumar, C.W. Yi, D.W. Goodman, Science 310 (2005) 291.
[10] F. Gao, Y.L. Wang, D.W. Goodman, J. Am. Chem. Soc. 131 (2009) 5734.
[11] A.M. Venezia, L.F. Liotta, G. Pantaleo, G. Deganello, A. Beck, Zs. Koppany, K. Frey, D. Horvath, L. Guczi, Appl. Catal. A 251 (2003) 359.
[12] N. Dimitratos, F. Porta, L. Prati, Appl. Catal. A 291 (2005) 210.
[13] D. Wang, A. Villa, F. Porta, D. Su, L. Prati, Chem. Commun. (2006) 1956.
[14] W.C. Ketchie, M. Murayama, R.J. Davis, J. Catal. 250 (2007) 264.
[15] N. Dimitratos, J.A. Lopez-Sanchez, D. Morgan, A.F. Carley, R. Tiruvalam, C.J. Kiely, D. Bethell, G.J. Hutchings, Phys. Chem. Chem. Phys. 11 (2009) 5142.
[16] J. Rebelli, M. Detwiler, S.G. Ma, C.T. Williams, J.R. Monnier, J. Catal. 270 (2010) 224.
[17] F. Cárdenas-Lizana, S. Gómez-Quero, A. Hugon, L. Delannoy, C. Louis, M.A. Keane, J. Catal. 262 (2009) 235.
[18] K. Qian, W.X. Huang, Z.Q. Jiang, H.X. Sun, J. Catal. 248 (2007) 137.
[19] K. Qian, W.X. Huang, J. Fang, S.S. Lv, B. He, Z.Q. Jiang, S.Q. Wei, J. Catal. 255 (2008) 269.
[20] K. Qian, H.X. Sun, W.X. Huang, J. Fang, S.S. Lv, B. He, Z.Q. Jiang, S.Q. Wei, Chem. Eur. J. 14 (2008) 10595.
[21] K. Qian, Z.Q. Jiang, W.X. Huang, J. Mol. Catal. A 264 (2007) 26.
[22] B. Pawelec, A.M. Venezia, V. La Parola, E. Cano-Serrano, J.M. Campos-Martin, J.L.G. Fierro, Appl. Surf. Sci. 242 (2005) 380.
[23] Z.H. Suo, C.Y. Ma, M.S. Jin, T. He, L.D. An, Catal. Commun. 9 (2008) 2187.
[24] F. Gao, Y. Wang, Y. Cai, D.W. Goodman, J. Phys. Chem. C 113 (2009) 174.
[25] N.S. Babu, N. Lingaiah, R. Gopinath, P.S.S. Reddy, P.S.S. Prasad, J. Phys. Chem. C 111 (2007) 6447.
[26] F. Gao, Y. Wang, D.W. Goodman, J. Phys. Chem. C 113 (2009) 14993.
[27] F. Gao, Y. Wang, D.W. Goodman, J. Phys. Chem. C 114 (2010) 4036.